12 September 2021

Applying Laplacian Magic Mirror in Freeform Illumination Optics Tolerancing

Wooyoun Kim, Jannick P. Rolland (/profile/Jannick.Rolland-5671), William J. Cassarly (/profile/William.Cassarly-20169)

Author Affiliations + ()

Proceedings Volume 11874, Illumination Optics VI; (/conference-proceedings-of-spie/11874.toc) 118740P (2021) https://doi.org/10.1117/12.2596898 (https://doi.org/10.1117/12.2596898)
Event: SPIE Optical Systems Design (/conference-proceedings-of-spie/browse/SPIE-Optical-Systems-Design/2021), 2021, Online Only

Abstract

Tolerance analysis is an integral part of the design process that saves time and money while improving the product quality. Nevertheless, tolerancing of illumination optics is often glossed over by the current industry. Consequently, there is a need to understand and establish tolerancing in illumination optics. This research focuses on single surface deformation. In the process referred to as surface perturbation, the surface is perturbed by a known amount. Then, the changes on the irradiance target are evaluated. A localized surface perturbation, like a bump or hole, results in either a local increase in irradiance with an annulus dip around the elevated irradiance or a local decrease in irradiance with an annulus increase around the decreased irradiance. Such an outcome is a result of flux conservation. The ratio between the height and the surface area (referred to as the size) of the localized surface perturbation has an approximately linear relationship to the largest irradiance change. Once the linearity of the relationship is understood for the localized surface perturbation of a particular size, the tolerance range can be estimated for other localized surface perturbations sizes. Within the optics' tolerancing range, the Laplacian of the surface perturbation predicts the irradiance change. As long as the ray-mapping between the surface and the target is known, the Laplacian of the surface change can be mapped onto the target. The surface change also perturbs the ray-mapping. Thus, taking the perturbed ray-mapping into account enables prediction with greater accuracy. Using this method, expected surface deformation from the manufacturing process can guide estimating irradiance changes, providing a first-order method to tolerance illumination optics.

Conference Presentation

KEYWORDS
Tolerancing
Freeform optics
Mirrors
Optics manufacturing

Show Transcript

ARTICLE | FIGURES & TABLES | REFERENCES | CITED BY

Ray tracing

Reflectors

Singular optics

WATCH PRESENTATION (/ebook/download?urlId=10.1117/12.2596898&isFullBook=false)

SAVE TO MY LIBRARY (/ebook/download?urlId=&isFullBook=false)

RELATED CONTENT

Toleranced freeform optical design with extended sources using ray targeting (/conference-proceedings-of-spie/8842/88420L/Toleranced-freeform-optical-design-with-extended-sources-using-ray-targeting/10.1117/12.2024969.full)
Proceedings of SPIE (September 30 2013)

Design of a two mirror telescope using a free form... (/conference-proceedings-of-spie/11057/110571T/Design-of-a-two-mirror-telescope-using-a-free-form/10.1117/12.2534326.full)
Proceedings of SPIE (June 21 2019)

Design of an ultra thin near eye display with geometrical... (/conference-proceedings-of-spie/10126/101260R/Design-of-an-ultra-thin-near-eye-display-with-geometrical/10.1117/12.2253301.full)
Proceedings of SPIE (February 16 2017)

Laser beam shaping by double tailoring (/conference-proceedings-of-spie/5876/587607/Laser-beam-shaping-by-double-tailoring/10.1117/12.616652.full)
Proceedings of SPIE (August 23 2005)

Specifications For Metal Optics (/conference-proceedings-of-spie/181/0000/Specifications-For-Metal-Optics/10.1117/12.957348.full)
Proceedings of SPIE (September 07 1979)

Concept and application of virtual normal surface (/conference-proceedings-of-spie/5638/0000/Concept-and-application-of-virtual-normal-surface/10.1117/12.573847.full)
Proceedings of SPIE (February 10 2005)

1. INTRODUCTION

Due to the high number of adjustable degrees of freedom and the lack of rotational symmetry, non-imaging freeform optics are used to create complex, customized illuminance ... would not be feasible with conventional optics. Particularly in design and production, major prog... de[1] (/conference-proceedings-of-spie/11874/2596898/Applying-Laplacian-Magic-Mirror-in-Freeform-Illumination-Optics-Tolerancing/10.1117/12.2596898.full#B1). Thus, several algorithms for the design of freeform optics already exist that determine the required optical surface from an arbitrary initial and the desired target illuminance distribution while taking ideal sources[2] (/conference-proceedings-of-spie/11874/2596898/Applying-Laplacian-Magic-Mirror-in-Freeform-Illumination-Optics-Tolerancing/10.1117/12.2596898.full#B2), 3 (/conference-proceedings-of-spie/11874/2596898/Applying-Laplacian-Magic-Mirror-in-Freeform-Illumination-Optics-Tolerancing/10.1117/12.2596898.full#B3) (zero etendue, e.g. point sources or collimated light) as well as extended sources[4] (/conference-proceedings-of-spie/11874/2596898/Applying-Laplacian-Magic-Mirror-in-Freeform-Illumination-Optics-Tolerancing/10.1117/12.2596898.full#B4), 5 (/conference-proceedings-of-spie/11874/2596898/Applying-Laplacian-Magic-Mirror-in-Freeform-Illumination-Optics-Tolerancing/10.1117/12.2596898.full#B5) into account. Moreover, additional functionalities, as a second source or target distribution, are achieved by special algorithms[6] (/conference-proceedings-of-spie/11874/2596898/Applying-Laplacian-Magic-Mirror-in-Freeform-Illumination-Optics-Tolerancing/10.1117/12.2596898.full#B6), 7 (/conference-proceedings-of-spie/11874/2596898/Applying-Laplacian-Magic-Mirror-in-Freeform-Illumination-Optics-Tolerancing/10.1117/12.2596898.full#B7).

However, almost all methods do not consider the expansion of the optics, so that, depending on the application, thick lenses are designed, which either exceed the available space or are simply not or too expensive to manufacture. During injection molding, for example, the cooling time correlates in square with component thickness and likewise the costs increase[8] (/conference-proceedings-of-spie/11874/2596898/Applying-Laplacian-Magic-Mirror-in-Freeform-Illumination-Optics-Tolerancing/10.1117/12.2596898.full#B8).

For conventional optics this problem is solved by Fresnel lenses which reduces the optics' size by segmentation along concentric circles (see figure 1 (/conference-proceedings-of-spie/11874/2596898/Applying-Laplacian-Magic-Mirror-in-Freeform-Illumination-Optics-Tolerancing/10.1117/12.2596898.full#F1)). In case of freeform optics, however, this approach is typically not applicable through the lack of rotational symmetry, so that a segmentation along concentric circles results in unnecessarily thick segmented lenses because the contour lines of constant height deviates significantly from this shape. Therefore, different strategies, as using a 2D array of prisms or lens-facets, were developed in the past[9] (/conference-proceedings-of-spie/11874/2596898/Applying-Laplacian-Magic-Mirror-in-Freeform-Illumination-Optics-Tolerancing/10.1117/12.2596898.full#B9), 10 (/conference-proceedings-of-spie/11874/2596898/Applying-Laplacian-Magic-Mirror-in-Freeform-Illumination-Optics-Tolerancing/10.1117/12.2596898.full#B10). In contrast to Fresnelization these approaches lead to more discontinuities at the boundaries of each element, which lead to a reduction in optical performance and are subject to greater manufacturing boundary conditions than continuous surfaces. Also for Fresnelized lenses the loss of optical performance is caused by optically unusable areas between the segments, further called "draft surfaces" (see figure 1 (/conference-proceedings-of-spie/11874/2596898/Applying-Laplacian-Magic-Mirror-in-Freeform-Illumination-Optics-Tolerancing/10.1117/12.2596898.full#F1)), which leads to radiation deflection (scattering) in deviating directions compared to the non-segmented surface. Due to deviations from the ideal shape caused by the manufacturing process, e.g. the finite size of the used tools, the optical unusable areas increase. In addition, the proportion of scattered light increases with the number of segments and the scattering effects can dominate the optical functionality.

Figure 1. Download (/proceedings/DownloadFigures?url=/ContentImages/Proceedings/11874/118740P/FigureImages/00031_psisdg11874_118740p_page_2_1.jpg)

Structure of a Fresnel lens. Possible parameters in the design of a Fresnel lens as well as the optical not usable area at the segment boundaries are shown. The latter deflects the light in other directions than the continuous optic and thus creates "scattering effects".

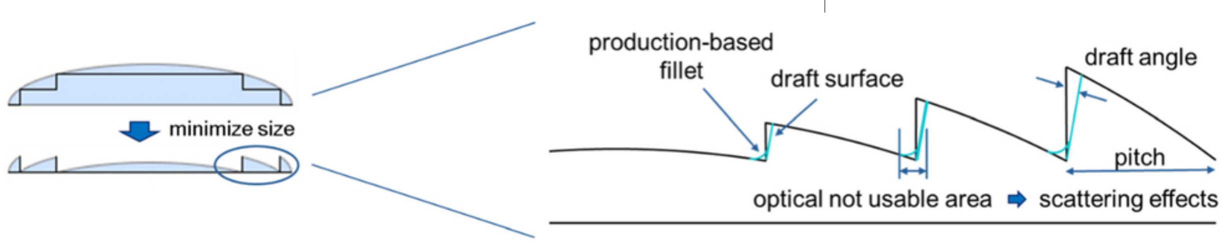

Using ideal light sources, there is only one ray direction in each point, so that the scattering effect can be reduced by changing the angle of the draft surfaces by aligning these parallel to the incoming rays. Simultaneously, a segmentation along concentric contour lines allows the thickness of the segments to be adjusted. The only approach known to the authors using this strategy to construct a Fresnel lens from a set of freeform optics by the incoming wavefront is done by Desnijder et all.[11] (/conference-proceedings-of-spie/11874/2596898/Applying-Laplacian-Magic-Mirror-in-Freeform-Illumination-Optics-Tolerancing/10.1117/12.2596898.full#B11).

However, this approach cannot be used for extended sources, where the light direction at each point propagates is not unique. Additionally, the fabrication boundary conditions are also neglected in this approach. In particular, complex contour lines can lead to problems in fabrication and a minimum or constant angle of attack of the draft surface, the draft angle, must be maintained to enable fabrication by diamond turning or a clean impression during injection molding.

In this work, a method is presented to design a Fresnel lens from a given freeform optic by optimizing the segmentation parameters as draft angle, pitch and fillet to reduce the effect due to the segmentation on the illuminance distribution by scattering effects while taking care of manufacturing conditions. In the presented approach, the adaptation of the parameters is based on optimization of the simulated illuminance distribution of the segmented freeform optic. With state-of-the-art ray tracing algorithms, the ...n number of segments as well as the complex structure lead to a considerable computational effort. Therefore, to accelerate the simulations of the illuminance distribution for the optimization, a specialized ray tracer is developed in a first step which considers the specific structure of segmented freeform optics. This simulation approach is subsequently used for the optimization of the Fresnelization parameters by an adapted evolutionary algorithm. The method's performance is illustrated on a lens for a head-up-display (HUD), where a display in front of the segmented lens always creates a moiré pattern whose effects are reduced by adjusting the Fresnelization parameters.

2. METHODS

The developed method for the design and optimization of Fresnelized freeform optics consists of two main components. One is simulation of the illumination distribution by ray tracing to evaluate the optical functionality of a given Fresnelized freeform optic and the other is the optimization algorithm itself. Since the simulations of the illumination he basis for the opt mization and the structures of Fresnelized freeform optics are very complex, the is

a. Simulation of the illumination distribution by ray tracing

Ray tracing is based on geometric optics to simulate the propagation of light. Therein, the light is considered as rays and the deflection of the rays at different objects from the source up to a screen or detector is calculated by Fresnel equations and the law of reflection. During this process most of the computing power is used to calculate the intersectic points between rays and objects. Therefore, ray tracing is much more efficient for simple objects such as spheres or cuboids than for complex geometries, where the intersection point can only be calculated numerically. In addition, if several objects are present, the correct object for the next intersection point of a ray must be determined first. Unless the order of the objects is specified, either all objects can be checked for intersection, which is very time-consuming, or acceleration structures can be used to speed up this process[1 (/conference-proceedings-of-spie/11874/2596898/Applying-Laplacian-Magic-Mirror-in-Freeform-Illumination-Optics-Tolerancing/10.1117/12.2596898.full#B12), 13 (/conference-proceedings-of-spie/11874/2596898/Applying-Laplacian-Magic-Mirror-in-Freeform-Illumination-Optics-Tolerancing/10.1117/12.2596898.full#B13)]. The more rays are used, the larger the advantage of such acceleration structures, since the effort for their initialization is reduced in relation to the reduction of the computational effort for a single ray. Most strategies for the acceleration structures are based on two general approaches which either use hierarchical bounding volumes or space partitioning[12 (/conference-proceedings-of-spie/11874/2596898/Applying-Laplacian-Magic-Mirror-in-Freeform-Illumination-Optics-Tolerancing/10.1117/12.2596898.full#B12), 13 (/conference-proceedings-of-spie/11874/2596898/Applying-Laplacian-Magic-Mirror-in-Freeform-Illumination-Optics-Tolerancing/10.1117/12.2596898.full#B13)]. In special cases, more specific acceleration structures can be adapted, thus increasing computation efficiency. A spherical Fresnel lens, for example, can be described by a CAD model or, to speed up the ray tracing, as a composition of spheres, cones and tori with varying center and radii. The simulation of the illuminance distribution of the segmented freeform optics, on the other hand, is considerably more complex.

In the following, the model for the Fresnel lens is created from a continuous B-Spline representation of the freeform surface by segmentation along predefined flat curves. By creating the Fresnel lens from only one surface the change of the optical path through the segmentation is neglected. In the presented method, segmentation can be performed along contour lines, but it can also deviate from them to account for manufacturing constraints by concentrically scaling a single, two-dimensional curve. From this two-dimensional curves three-dimensional uniform B-Spline curves are constructed which divide the continuous freeform surface into segments and these moreover into partial surfaces, which are parts of the continuous freeform surface, the draft surfaces and, if desired, fillets. So that, for each border of a partial surface a boundary curve is created. To simplify the subsequent ray tracing, the knot vectors for the uniform B-Splines describing these curves are created with a common, monotonously increasing polar angle. Then draft surfaces and fillets are created from these curves using the same angle dependencies. To reduce the computational effort during the creation of the model as well as during the ray tracing, the freeform surface itself is not segmented. Instead, only the offset of the freeform surface for each segment is determined by the created curves to shift the rays later. On the backside, the lens is bounded by a flat surface.

Due to the complex structure of the model, adapted acceleration structures are required for the efficient ray tracing of Fresnelized freeform optics. One possibility for space partitioning is based on a 3-dimensional grid of voxels (3d-pixels), where for each voxel the contained optical elements are stored[12 (/conference-proceedings-of-spie/11874/2596898/Applying-Laplacian-Magic-Mirror-in-Freeform-Illumination-Optics-Tolerancing/10.1117/12.2596898.full#B12)]. In case of Fresnelized freeform optics, the individual partial surfaces have a ring-like structure, so that the spatial extent is relatively large compared to the ring width. Using the z-axis as propagation direction, this is especially true in the x-y plane for the draft surfaces (at a small draft angle) and for the fillets additionally also in the z-direction, if segmentation deviates from a segmentation along the contour lines. In order to resolve the individual partial surfaces, a very detailed grid would be required. This can then lead to a high initialization overhead, which still results in significant computation time even if the number of rays is low.

To enable efficient ray tracing, a combined approach is used in this work to simulate the illuminance distribution of Fresnelized freeform optics, which makes use of voxels and additionally exploits the special structure of Fresnel optics. Instead of initializing a very detailed voxel grid or checking multiple partial surfaces in a less detailed voxel grid, it takes advantage of the fact that the individual partial surfaces of a Fresnel lens do not overlap and are lined up in a fixed order. Using this, as well as the special polar angle dependencies of the constructed B-Spline knot vectors, voxel grids are only necessary for the boundary curves and for the continuous freeform surface.

Since the intersection of rays and surface is determined numerically, the efficiency of the ray-surface intersection depends on the used starting point for the ray position and the B-Spline parameters, so that the voxel grid for the continuous freeform surface can be used in double function. Therefore, not only the information, if the surface intersects a voxe is stored but also a pair of B-Spline parameters which corresponds to a point on the surface inside the voxel is additionally stored for each voxel containing a part of the surface. Due to the systematic structure of the curves, no corresponding B-Spline parameter information is required for the curves, because the B-Spline parameter for the starting point can already be determined by the angle due to the construction of the knot vector. Therefore, the resolution of the voxel grids for the curves can be significantly lower as the one for the freeform surface which must only be calculated once in the whole computation.

In addition to the grid for the freeform surface, two or, with filleting, three further two-dimensional grids are created. These grids store the segment number at each node (corner o voxel) for a certain sort of curves (e.g. the curves which belong to the edge of the draft surfaces and to parts of the freeform surface). While the creation of the grid for the freeforr surface is independent of the number of segments, the resolution of those grids should be in the order of magnitude of the employed segments.

With the help of the constructed grids, the raytracing is accelerated. To explain the principle, a simplified case is considered first. Assume that a ray is reflected at the inner side o an optical system segmented along contour lines, so that, in addition to the current position and direction of the ray, the partial surface of the last intersection point is also known.

Thus, the number of partial surfaces, which come into question for the next intersection with this ray, is reduced considerably by utilizing geometric considerations (see figure 2 (/conference-proceedings-of-spie/11874/2596898/Applying-Laplacian-Magic-Mirror-in-Freeform-Illumination-Optics-Tolerancing/10.1117/12.2596898.full#F2)). From the remaining partial surfaces, the correct surface for the next intersection is determined by the intersection point of the two dimensional projection in the x-y plane of the ray with the neighboring boundary curves, as well as the relation of the actual heights of the ray and the curve at this point (above or below). For segmentations that deviate from a ...ong contour lines, in some cases more ray-curve intersections are necessary due to the deviatin...

Figure 2. Download (/proceedings/DownloadFigures?url=/ContentImages/Proceedings/11874/118740P/FigureImages/00031_psisdg11874_118740p_page_4_1.jpg)

Visualization of the limited intersection possibilities depending on the surface of the last intersection.

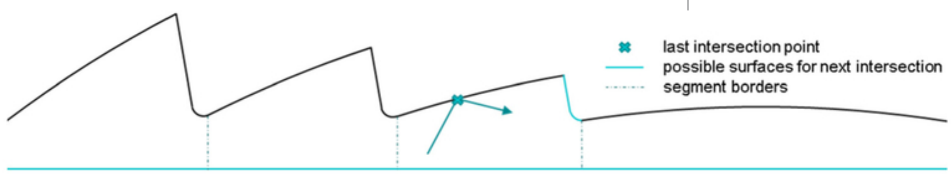

For incoming rays, which are already deflected at the plane bottom, the last intersection point cannot be used to reduce the number of partial surfaces as in the simplified case, because of the comparably large extent of this surface. Therefore, the ray is traced to a plane closely before the Fresnel structures and from the intersection point of the ray with this plane the segment number is determined by the previously created two-dimensional grids. Based on the deviations of the segment numbers in the different grids, the number of partial surfaces is reduced, and the correct surface is determined by the boundary curves as explained for the simplified case. In addition, the obtained intersection points with the boundary curves provide a good approximation of the initial values in real and parameter space for the following ray-surface intersection calculation, which are also thereby reduced to the minimum.

b. Optimization

By optimizing the Fresnel lens, the scattering effects due to segmentation should be reduced and at the same time the manufacturability of the lens should be considered. For this reason, three objective functions are defined. The first function is used to minimize the effect due to the segmentation and therefore considers the illumination distribution. For this purpose, the quadratic deviation from a target distribution is utilized by:

$$f = \sum_i (I_i - I_{\text{target},\, i})^2 \qquad (1)$$

where I_i is the value of the tested and $I_{\text{target},\, i}$ the value of the target illumination distribution in each pixel i of the detector. To get as close as possible to the performance of the non-segmented lens with the Fresnel lens, its illuminance distribution can be used as the target distribution. To optimize the segmentation curves, the second objective function considers production constraints. For example, the cost of a lens or a mold produced by diamond turning depends on the manufacturing time which is determined from the maximum tool acceleration along the curve. Therefore, the maximum acceleration is used as second objective function in this case. The last optimization function considered is the height of the segmented optics. This is calculated by the model of the Fresnel lens used during ray tracing.

To ensure that other parameters, such as manufacturing parameters or segment height, can be considered independently in addition to the illuminance distribution during the optimization, a multi-objective function optimization, a so-called Pareto optimization, is used. Employing a multi-objective function optimization instead of a single solution the Pareto front is approximated, which is a curve or surface of points which cannot be improved in one objective function without deteriorating another one. For a Pareto optimization evolutionary algorithms can be used, where many individuals, each a set of parameters, are used for the optimization, which are combined and mutated, mimicking natural evolution. Then the optimization result is given by the individuals which are nondominated, which means that no other individual has a better value in all objective functions. For the optimization, a slightly adapted NSGA-II algorithm[14 (/conference-proceedings-of-spie/11874/2596898/Applying-Laplacian-Magic-Mirror-in-Freeform-Illumination-Optics-Tolerancing/10.1117/12.2596898.full#B14)] is used in this work.

3. RESULTS

For the demonstrator of the head-up display (HUD), a rectangular freeform lens (ca. 80x50mm^2) is considered which is uniformly illuminated by a divergent source. The combination of the segmented lens with a display mounted behind of it creates a moiré pattern in the illuminance distribution. This pattern is an optical effect which is created by the superposition of two regular patterns and varies with a change in pitch, displacement or rotation of the two patterns. Therefore, the moiré effect is to be reduced by adjusting the Fresnelization parameters. For manufacturing reasons, in addition to Fresnelization along the approximately elliptical contour lines, segmentation based on circles as well as a combination of both curves can in principle be considered. However, with otherwise identical parameters, even a small deviation of the segmentation lines from the contour lines (ratio of the semi-axes approx. 0.75) leads to a significantly thicker Fresnel lens (about a 5-fold height with a ratio of the semi-axes of 0.8). For this reason, only segmentation along contour lines is considered in this application. A constant pitch is chosen for Fresnelization, which shall lie between 150µm and 300µm. This corresponds to approximately between 160 and 330 segments. The draft angle is assumed to be at least 5° for manufacturing reasons and it is limited to maximal 40° upwards during optimization.

...oiré pattern, the resolution of the illum nance distribution must be many times higher than the pit... the ... Therefore ...bout 25µm is chosen for the illuminance distribution. Due to the high resolution of the illuminance distribution and due to the display, which absorbs 80% of the radiation, 300 million rays are used which still results in noise in the Monte Carlo ray tracing that has about the same order of magnitude as the moiré pattern. Nevertheless, the simulated illuminance distribution represents a good compromise in terms of computational effort. The specially developed ray tracer needs about 25s to create the model of the Fresnel lens and about 15 minutes for the complete ray tracing with a 2.6 GHz Intel Xenon Gold 6240M. For smaller amounts of rays, the computing time for raytracing decrease: accordingly, e.g. the raytracing of 10 million rays needs 25s, which makes in total about 50s for the whole simulation.

Because the moiré pattern is observed directly behind the display whose position depends on the thickness of the lens, using the illuminance distribution of the non-segmented lens is only suitable for reducing it to a limited extent. Due to the different thicknesses of the segmented (<100µm) and the non-segmented (a few mm) lenses, the changed position of the detector has a greater effect on the illuminance distribution than the moiré pattern (see figure 3 (/conference-proceedings-of-spie/11874/2596898/Applying-Laplacian-Magic-Mirror-in-Freeform-Illumination-Optics-Tolerancing/10.1117/12.2596898.full#F3) left). For this reason, the target distribution is created by the average of different randomly selected illuminance distributions in the selected parameter space for pitch and draft angle, so that no moiré pattern appears in the target distribution.

Figure 3. Download (/proceedings/DownloadFigures?url=/ContentImages/Proceedings/11874/118740P/FigureImages/00031_psisdg11874_118740p_page_5_1.jpg)

Illuminance distribution in front of the non-segmented lens (left) and the target distribution for optimization (right).

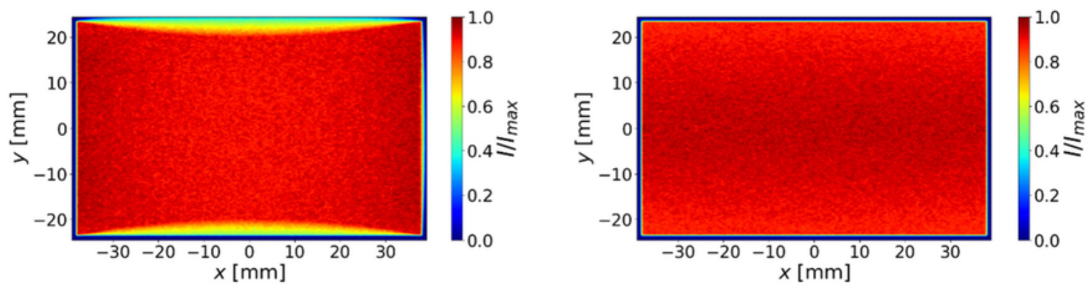

In figure 4 (/conference-proceedings-of-spie/11874/2596898/Applying-Laplacian-Magic-Mirror-in-Freeform-Illumination-Optics-Tolerancing/10.1117/12.2596898.full#F4) the two individuals of the optimization with the lowest function value for each of the two objective functions are presented. For both, the draft angle is close to the minimum value of 5° an the pitch is 150µm and 191µm respectively. The latter has the lower deviation to the target illuminance distribution (first objective function) while, as expected, the minimal height occurs at the smallest possible pitch. Also, the other dominating individuals cluster closely around these values. Comparing the two illuminance distributions, a rapidly oscillating moiré pattern can be seen in both, which has about the same order of magnitude but is curved in different directions (toward and away from the center of the image, respectively) Although, the value of the first objective function is twice as high for the thinner lens, the perception of the moiré pattern is quite similar for both so that in this case the thinner len: is chosen as final result of the optimization.

Figure 4. Download (/proceedings/DownloadFigures?url=/ContentImages/Proceedings/11874/118740P/FigureImages/00031_psisdg11874_118740p_page_6_1.jpg)

Optimization results with minimal height (left) and minimal scattering effect (right). The left has a pitch of 150µm and 5.4° draft angle, which results in a height of 70µm and f = 1.4% f_{max}. The higher pitch of the right (191µm) with almost same angle (also 5.4°) results in a slightly thicker lens (height of 78µm) but a smaller value of the first objective function (f = 0.8% f_{max}).

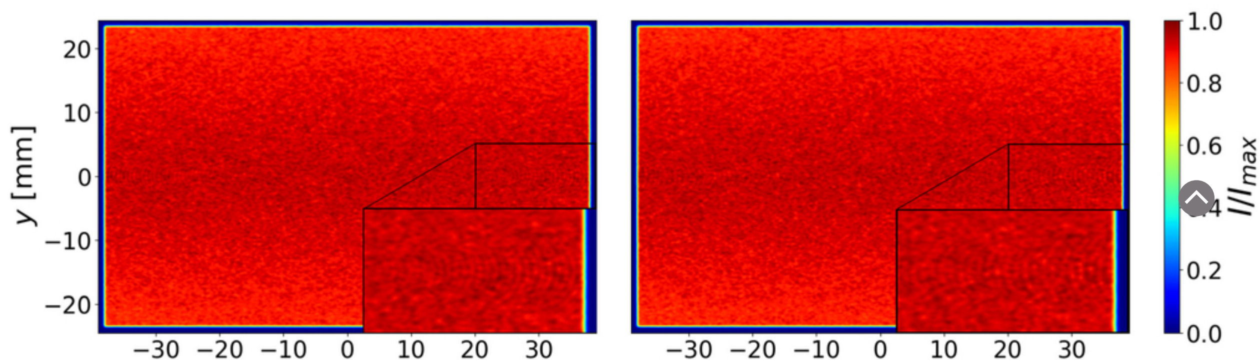

To evaluate the results of the optimization, the dependencies of the first objective function, which is based on the illuminance distribution through equation (1) (/conference-proceedings-of-spie/11874/2596898/Applying-Laplacian-Magic-Mirror-in-Freeform-Illumination-Optics-Tolerancing/...#d1) are ...rately below. Figure 5 (/conference-proceedings-of-spie/11874/2596898/Applying-Laplacian-Magic-Mirror-in-Freeform-Illumination-Optics-Tolerancing/10.1117/12.2596898.full#F5) shows a varying pitch at a constant draft angle of 5°, as well as the dependence of the illuminance distribution on the draft angle at a pitch of 220µm.

Figure 5. Download (/proceedings/DownloadFigures?url=/ContentImages/Proceedings/11874/118740P/FigureImages/00031_psisdg11874_118740p_page_6_2.jpg)

Normalized function values of the first objective function (based on the simulation of the illuminance distribution) depending on the pitch by a constant draft angle of 5° (left) and depending on the draft angle with a constant pitch of 220µm (right).

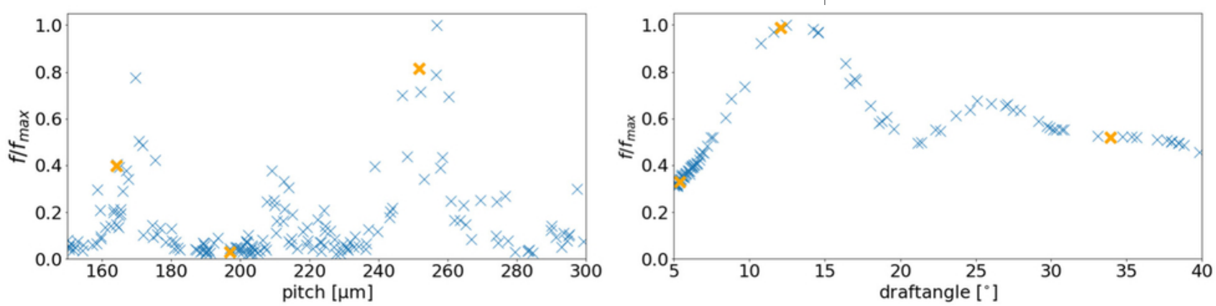

In the distribution of illuminance versus pitch, there are some domains that have particularly low values (for example, around 150µm, 190µm, 230µm and 280µm) but also domains that have a significantly higher value. The high function values coincide with domains with a low frequency of the moiré pattern, which is more noticeable by an observer. The higher the frequency of the moiré pattern, the less it is perceived in the generated distributions. This matches the domains with low function values. To visualize this, figure 6 (/conference-proceedings-of-spie/11874/2596898/Applying-Laplacian-Magic-Mirror-in-Freeform-Illumination-Optics-Tolerancing/10.1117/12.2596898.full#F6) shows three examples which are also highlighted in figure 5 (/conference-proceedings-of-spie/11874/2596898/Applying-Laplacian-Magic-Mirror-in-Freeform-Illumination-Optics-Tolerancing/10.1117/12.2596898.full#F5). Therefore, the value of the first objective function correlates with the perception of the moiré pattern of an observer. Nevertheless, there is a noise-like variation over the entire curve, which can possibly be explained by the discontinuities of the Fresnel lens.

Figure 6. Download (/proceedings/DownloadFigures?url=/ContentImages/Proceedings/11874/118740P/FigureImages/00031_psisdg11874_118740p_page_7_1.jpg)

Examples for the Moiré pattern with constant draft angle. From left to right: 164µm (f = 40% f_{max}), 197µm (f = 3% f_{max}), 252µm (f = 82% f_{max}).

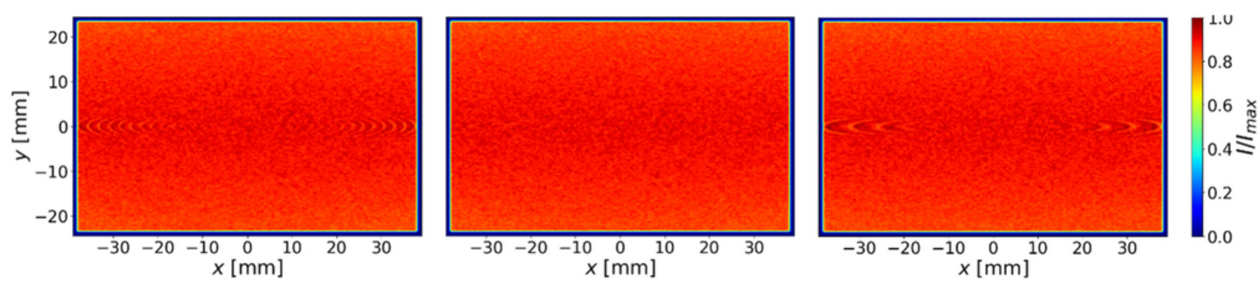

The dependency of the first objective function on the draft angle shows a low value especially at small draft angles, but it also decreases again with increasing draft angle exhibiting a peak around 10 – 15°. This also agrees with the visual perception of the moiré pattern. At small draft angles, the optical unusable area is smaller and so is the moiré pattern. At sufficiently large draft angles, however, the distribution of light in the illumination distribution changes at the observed distance, so that the edge region is less strongly illuminated and thus the moiré pattern is less strongly perceived (cf. figure 7 (/conference-proceedings-of-spie/11874/2596898/Applying-Laplacian-Magic-Mirror-in-Freeform-Illumination-Optics-Tolerancing/10.1117/12.2596898.full#F7) and, highlighted datapoints in figure 5 (/conference-proceedings-of-spie/11874/2596898/Applying-Laplacian-Magic-Mirror-in-Freeform-Illumination-Optics-Tolerancing/10.1117/12.2596898.full#F5)).

Figure 7. Download (/proceedings/DownloadFigures?url=/ContentImages/Proceedings/11874/118740P/FigureImages/00031_psisdg11874_118740p_page_7_2.jpg)

Examples for the Moiré pattern with constant draft angle. From left to right: 5.4° (f = 33% f_{max}), 12.1° (f = 98% f_{max}), 34.0° (f = 52% f_{max}).

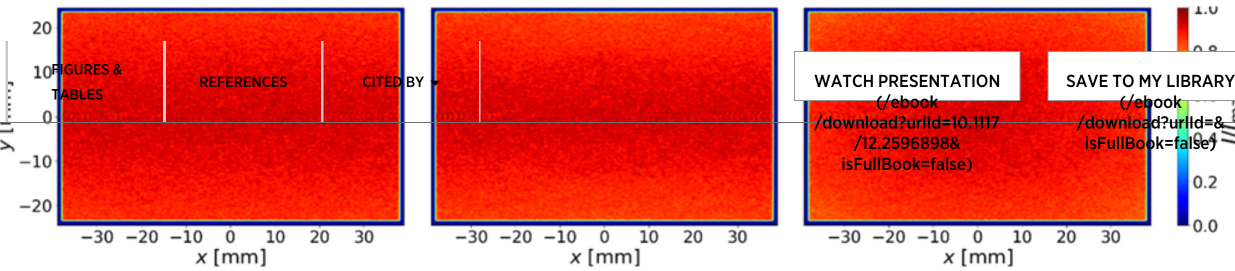

4. SUMMARY

In this work a method for the optimized segmentation of Fresnelized freeform optics is presented. For this purpose, a specialized ray tracer is developed for the simulation of the illuminance distribution of segmented freeform optics. This considers the special geometry of Fresnel lenses and therefore enables an efficient construction of acceleration structures and an efficient raytracing. This enables the optimization of the Fresnelization parameters such as pitch and draft angle. Using the specialized ray tracer, the Fresnelization parameters pitch and draft angle are optimized for the selected example of a HUD to reduce the moiré pattern caused by the upstream display while concerning th height of the Fresnel lens. To evaluate the optimization result, the dependence of the moiré pattern on pitch and draft angle is also considered and the perception of the moiré pattern is compared with the value of the objective function, which rates the illuminance distribution. Here, a correlation between the perception of the moiré pattern with the objective function is found. In future work, a more specialized objective function for the evaluation of the illuminance distribution might be developed which minimizes the noise-lik variations in the dependency on pitch and so may result in a more stable optimization. Moreover, on further applications the simultaneous optimization of the segmentation curve due to manufacturing constraints will be evaluated.

ACKNOWLEDGMENTS

The authors thank the German Federal Ministry of Education and Research for funding within the project “FRESNELOPT” (No. 13N14707). Jacqueline Dahlmanns is part of the Max Planck School of Photonics supported by BMBF, Max Planck Society, and Fraunhofer Society.

REFERENCES

[1] Wu, R., Feng, Z., Zheng, Z., Liang, R., Benítez, P., Miñano, J. C. and Duerr, F., “Design of Freeform Illumination Optics,” Laser & Photonics Reviews, 12 (7), 1700310 (2018) https://doi.org/10.1002/lpor.v12.7 (https://doi.org/10.1002/lpor.v12.7) Google Scholar (http://scholar.google.com/scholar_lookup?title=Design+of+Freeform+Illumination+Optics&author=R.+Wu&author=Z.+Feng&author=Z.+Zheng&author=R.+Liang&author=P.+Benítez&author=J.+C.+Miñano&author=F.+Duerr&journal=Laser+&+Photonics+Reviews&volume=12&issue=7&publication_year=2018&pages=1700310)

[2] Oliker, V., “Controlling light with freeform multifocal lens designed with supporting quadric method(SQM),” Optics express, 25 (4), A58 –A72 (2017). https://doi.org/10.1364/OE.25.000A58 (https://doi.org/10.1364/OE.25.000A58) Google Scholar (http://scholar.google.com/scholar_lookup?title=Controlling+light+with+freeform+multifocal+lens+designed+with+supporting+quadric+method(SQM)&author=V.+Oliker&journal=Optics+express&volume=25&issue=4&publication_year=2017&pages=A58-A72)

[3] Bäuerle, A., Bruneton, A., Wester, R., Stollenwerk, J. and Loosen, P., “Algorithm for irradiance tailoring using multiple freeform optical surfaces,” Optics express, 20 (13), 14477 –14485 (2012). https://doi.org/10.1364/OE.20.014477 (https://doi.org/10.1364/OE.20.014477) Google Scholar (http://scholar.google.com/scholar_lookup?title=Algorithm+for+irradiance+tailoring+using+multiple+freeform+optical+surfaces&author=A.+Bäuerle&author=A.+Bruneton&author=R.+Wester&author=J.+Stollenwerk&author=P.+Loosen&journal=Optics+express&volume=20&issue=13&publication_year=2012&pages=14477-14485)

[4] Völl, A., Berens, M., Wester, R., Buske, P., Stollenwerk, J. and Loosen, P., “Freeform optics design for extended sources in paraxial approximation exploiting the expectation maximization algorithm,” Optics express, 28 (24), 37004 –37014 (2020). https://doi.org/10.1364/OE.412541 (https://doi.org/10.1364/OE.412541) Google Scholar (http://scholar.google.com/scholar_lookup?title=Freeform+optics+design+for+extended+sources+in+paraxial+approximation+exploiting+the+expectation+maximization+algorithm author=A.+Völl&author=M.+Berens&author=R.+Wester&author=P.+Buske&author=J.+Stollenwerk&author=P.+Loosen&journal=Optics+express&volume=28& e=24& publication_year=2020&pages=37004-37014)

[5] Luo, Y., Feng, Z., Han, Y. and Li, H., “Design of compact and smooth free-form optical system with uniform illuminance for LED source,” Optics express, 18 (9), 9055 –9063 (2010). https://doi.org/10.1364/OE.18.009055 (https://doi.org/10.1364/OE.18.009055) Google Scholar (http://scholar.google.com

/scholar_lookup?title=Design+of+compact+and+smooth+free-form+optical+system+with+uniform+illuminance+for+LED+source&author=Y.+Luo&author=Z.+Feng&author=Y.+Han&author=H.+Li&journal=Optics+express&volume=18&issue=9&publication_year=2010&pages=9055-9063)

[6] Benítez, P., "Simultaneous multiple surface optical design method in three dimensions," Opt. Eng, 43 (7), 1489 (2004). https://doi.org/10.1117/1.1752918 (https://doi.org/10.1117/1.1752918) Google Scholar (http://scholar.google.com/scholar_lookup?title=Simultaneous+multiple+su…tez&journal=Opt.+Eng&volume=43&issue=7&publication_year=2004&pages=1489)

[7] Wu, X., Jin, G. and Zhu, J., "Freeform illumination design model for multiple light sources simultaneously," Applied optics, 56 (9), 2405 –2411 (2017). https://doi.org/10.1364/AO.56.002405 (https://doi.org/10.1364/AO.56.002405) Google Scholar (http://scholar.google.com/scholar_lookup?title=Freeform+illumination+design+model+for+multiple+light+sources+simultaneously&author=X.+Wu&author=G.+Jin&author=J.+Zhu&journal=Applied+optics&volume=56&issue=9&publication_year=2017&pages=2405-2411)

[8] Yu, C. J. and Sunderland, J. E., "Determination of ejection temperature and cooling time in injection molding," Polym. Eng. Sci., 32 (3), 191 –197 (1992). https://doi.org/10.1002/(ISSN)1548-2634 (https://doi.org/10.1002/(ISSN)1548-2634) Google Scholar (http://scholar.google.com/scholar_lookup?title=Determination+of+ejection+temperature+and+cooling+time+in+injection+molding&author=C.+J.+Yu&author=J.+E.+Sunderland&journal=Polym.+Eng.+Sci.&volume=32&issue=3&publication_year=1992&pages=191-197)

[9] Liu, L., Engel, T., Flury, M. and Visser, M. de, "Faceted structure: a design for desired illumination and manufacture using 3D printing," OSA Continuum, 1 (1), 26 (2018). https://doi.org/10.1364/OSAC.1.000026 (https://doi.org/10.1364/OSAC.1.000026) Google Scholar (http://scholar.google.com/scholar_lookup?title=Faceted+structure:+a+design+for+desired+illumination+and+manufacture+using+3D+printing&author=L.+Liu&author=T.+Engel&author=M.+Flury&author=M.+de+Visser&journal=OSA+Continuum&volume=1&issue=1&publication_year=2018&pages=26)

[10] Goldstein, P., "Process for designing a freeform Fresnel lens," Opt. Eng, 50 (12), 121703 (2011). https://doi.org/10.1117/1.3617474 (https://doi.org/10.1117/1.3617474) Google Scholar (http://scholar.google.com/scholar_lookup?title=Process+for+designing+a+freeform+Fresnel+lens&author=P.+Goldstein&journal=Opt.+Eng&volume=50&issue=12&publication_year=2011&pages=121703)

[11] Desnijder, K., Hanselaer, P. and Meuret, Y., "Freeform Fresnel lenses with a low number of discontinuities for tailored illumination applications," Optics express, 28 (17), 24489 –24500 (2020). https://doi.org/10.1364/OE.397983 (https://doi.org/10.1364/OE.397983) Google Scholar (http://scholar.google.com/scholar_lookup?title=Freeform+Fresnel+lenses+with+a+low+number+of+discontinuities+for+tailored+illumination+applications&author=K.+Desnijder&author=P.+Hanselaer&author=Y.+Meuret&journal=Optics+express&volume=28&issue=17&publication_year=2020&pages=24489-24500)

[12] Amanatides, J. and Woo, A., "A Fast Voxel Traversal Algorithm for Ray Tracing," 3 –10 North-Holland, Amsterdam (1987). Google Scholar (http://scholar.google.com/scholar_lookup?title=A+Fast+Voxel+Traversal+Algorithm+for+Ray+Tracing&author=J.+Amanatides&author=A.+Woo&publication_year=1987&pages=3-10)

[13] Lagae, A. and Dutré, P., "Compact, Fast and Robust Grids for Ray Tracing," Computer Graphics Forum, 27 (4), 1235 –1244 (2008). https://doi.org/10.1111/cgf.2008.27.issue-4 (https://doi.org/10.1111/cgf.2008.27.issue-4) Google Scholar (http://scholar.google.com/scholar_lookup?title=Compact,+Fast+and+Robust+Grids+for+Ray+Tracing&author=A.+Lagae&author=P.+Dutré&journal=Computer+Graphics+Forum&volume=27&issue=4&publication_year=2008&pages=1235-1244)

[14] Deb, K., Pratap, A., Agarwal, S. and Meyarivan, T., "A fast and elitist multiobjective genetic algorithm: NSGA-II," IEEE Trans. Evol. Computat., 6 (2), 182 –197 (2002). https://doi.org/10.1109/4235.996017 (https://doi.org/10.1109/4235.996017) Google Scholar (http://scholar.google.com/scholar_lookup?title=A+fast+and+elitist+multiobjective+genetic+algorithm:+NSGA-II&author=K.+Deb&author=A.+Pratap&author=S.+Agarwal&author=T.+Meyarivan&journal=IEEE+Trans.+Evol.+Computat.&volume=6&issue=2&publication_year=2002&pages=182-197)

Citation

Download Citation

Wooyoun Kim, Jannick P. Rolland (/profile/Jannick.Rolland-5671), and William J. Cassarly (/profile/William.Cassarly-20169) "Applying Laplacian Magic Mirror in Freeform Illumination Optics Tolerancing", Proc. SPIE 11874, Illumination Optics VI, 118740P (12 September 2021); https://doi.org/10.1117/12.2596898 (https://doi.org/10.1117/12.2596898)